Atmospheric Environment 179 (2018) 118–131

Contents lists available at ScienceDirect

Atmospheric Environment

journal homepage: www.elsevier.com/locate/atmosenv

Total dissolved atmospheric nitrogen deposition in the anoxic Cariaco basin

R. Rasse[a,b], T. Pérez[a,*], A. Giuliante[a], L. Donoso[a]

[a] Instituto Venezolano de Investigaciones Científicas, Centro de Ciencias Atmosféricas y Biogeoquímica, Laboratorio de Biogeoquímica, Aptdo, 20632, Caracas, 1020A, Venezuela

[b] Plymouth Marine Laboratory, Plymouth, UK

ABSTRACT

Atmospheric deposition of total dissolved nitrogen (TDN) is an important source of nitrogen for ocean primary productivity that has increased since the industrial revolution. Thus, understanding its role in the ocean nitrogen cycle will help assess recent changes in ocean biogeochemistry. In the anoxic Cariaco basin, the place of the CARIACO Ocean Time-Series Program, the influence of atmospherically-deposited TDN on marine biogeochemistry is unknown. In this study, we measured atmospheric TDN concentrations as dissolved organic (DON) and inorganic (DIN) nitrogen (TDN = DIN + DON) in atmospheric suspended particles and wet deposition samples at the northeast of the basin during periods of the wet (August–September 2008) and dry (March–April 2009) seasons. We evaluated the potential anthropogenic N influences by measuring wind velocity and direction, size-fractionated suspended particles, chemical traces and by performing back trajectories. We found DIN and DON concentration values that ranged between 0.11 and 0.58 μg-N m^{-3} and 0.11–0.56 μg-N m^{-3} in total suspended particles samples and between 0.08 and 0.54 mg-N l^{-1} and 0.02–1.3 mg-N l^{-1} in wet deposition samples, respectively. Continental air masses increased DON and DIN concentrations in atmospheric suspended particles during the wet season. We estimate an annual TDN atmospheric deposition (wet + particles) of 3.6 × 10^3 ton-N $year^{-1}$ and concluded that: 1) Atmospheric supply of TDN plays a key role in the C and N budget of the basin because replaces a fraction of the C (20% by induced primary production) and N (40%) removed by sediment burial, 2) present anthropogenic N could contribute to 30% of TDN atmospheric deposition in the basin, and 3) reduced DON (gas + particles) should be a significant component of bulk N deposition.

1. Introduction

The Cariaco basin is a semi-closed marine ecosystem with permanent anoxic conditions below 250 m depth (Muller-Karger et al., 2001). This basin is the place of the CARIACO Ocean Time-Series Program where carbon (C) and nitrogen (N) cycles have been studied since 1995 (e.g., Muller-Karger et al., 2001, 2004; 2010). In the basin, photosynthetic production of organic matter is driven by temporal changes in N content derived from upwelling, tributary rivers and atmospheric deposition (Muller-Karger and Castro, 1994; Muller-Karger et al., 2001, 2004; Thunell et al., 2007; Goñi et al., 2003). Until now, nitrogen derived from upwelling and rivers has been quantified (Bustamante et al., 2015; Muller-Karger et al., 2010); however, there is no information about the atmospheric N deposited on the sea surface of the basin.

Atmospheric nitrogen is deposited on the sea surface of the basin by dry (particles + gases) and wet (rainfall) deposition (e.g., Duce et al., 1991; Prospero et al., 1996). During dry and wet deposition, nitrogen is supplied in its insoluble and soluble forms (Duce et al., 1991, 2008; Jickells et al., 2017; Kanakidou et al., 2012; Neff et al., 2002). Total dissolved nitrogen (TDN) is the soluble form and encompasses dissolved inorganic (DIN: NH_4^+ + NO_3^-) and organic nitrogen (DON).

The role of TDN atmospheric deposition in marine C and N cycles has attracted increasing attention due to its enhancement since the industrial revolution (Duce et al., 2008; Ito et al., 2014, 2015; Jickells et al., 2017; Kanakidou et al., 2012; Kim et al., 2011, 2014; Dentener et al., 2006; Galloway et al., 2004, 2008; Singh et al., 2012). Particularly in semi-closed marine ecosystems near anthropogenic sources (e.g., Dentener et al., 2006; Duce et al., 2008; Jickells et al., 2017); where TDN atmospheric deposition can contribute to about 60% of primary production (Christodoulaki et al., 2013) and can replace 30% of the N removed by sediment burial (Teodoru et al., 2007). Therefore, quantifying TDN atmospheric deposition and its anthropogenic fraction would improve our understanding of the role of the atmosphere in the C and N cycles of the Cariaco basin.

It is challenging to assess the anthropogenic fraction of the atmospheric TDN because: 1) its organic fraction (DON) is poorly

* Corresponding author.
E-mail address: tperez@ivic.gob.ve (T. Pérez).

https://doi.org/10.1016/j.atmosenv.2018.02.007
Received 24 April 2017; Received in revised form 25 January 2018; Accepted 3 February 2018
Available online 06 February 2018
1352-2310/

characterized and 2) it is difficult partitioning anthropogenic and natural sources of TDN (Cape et al., 2011; Chen et al., 2010; Cornell et al. 2011a,b; Fischer et al., 2006; Jickells et al., 2013, 2017; Kanakidou et al., 2012; Mace et al., 2003a,b; Miyazaki et al., 2011; Neff et al., 2002; Zamora et al., 2011). Therefore, complementary measurements are required to identify the potential sources of TDN in wet deposition and atmospheric suspended particles (e.g., Cornell et al., 2001; Mace et al., 2003a,b; Pavuluri et al., 2015). For example, meteorological measurements and back trajectories are used to identify the origin of the air masses, whereas the collection of size-fractionated suspended particles is applied to separate atmospheric particles derived from different sources (Cornell et al., 2001; Jickells et al., 2013; Kumar and Sarin, 2010; Luo et al., 2016; Mace et al., 2003a,b; Qi et al., 2013; Violaki et al., 2015; Zamora et al., 2011). In addition, correlations between DIN, DON, and chemical tracers (e.g., non sea salt sulfate) in wet deposition and atmospheric suspended particles are applied to identify sources of TDN (Cape et al., 2005, 2011; Chen and Chen, 2010; Chen et al., 2010, 2015; Mace et al., 2003b; Lesworth et al., 2010; Zhang et al., 2008).

In this study, we measured DIN and DON (TDN = DIN + DON) and other chemical tracers (K^+, SO_4^{2-}, Mg^{2+} and Ca^{2+}) in wet deposition and atmospheric suspended particles at the northeast of Cariaco basin (Margarita Island, Fig. 1) during periods of the wet (August-September 2008) and dry (March-April 2009) seasons. Complementary meteorological measurements and back trajectories were also conducted. The goals of this study were: (1) To provide the first estimate TDN atmospheric deposition in the Cariaco basin and assess its role in the C and N cycles, and (2) to evaluate how anthropogenic N can impact the atmospheric supply of TDN in the basin.

2. Materials and methods

2.1. Sampling site and methods

The Cariaco basin is located in the continental margin of north Venezuela (Fig. 1). In this place, local air masses are derived from Jet stream winds while meteorological conditions (e.g., precipitation and wind velocity) are driven by the migration of the intertropical converging zone (ITCZ). Northward and southward migration of the ITCZ generates the wet and dry seasons between July–December and January–June, respectively. (Muller-Karger et al., 2010; Thunell et al., 2007). Therefore, to collect seasonal wet deposition and atmospheric suspended particles samples, we conducted two sampling campaigns at the northeast of the basin between August-September 2008 and March-April 2009 (Fig. 1).

2.1.1. Suspended particles in the atmosphere

Atmospheric suspended particles were collected on pre-combusted (400 °C) and pre-weighed glass fiber filters (GF/F). For the wet and dry season campaigns a total of 4 and 3 sampling periods (5–7 continuous days each) were performed, respectively. For statistical purposes we collected duplicates at each sampling time by using: 1) Two high-volume samplers (Hi-Vol, General Metal Works, model GMWL-200H) to collect total suspended particles (TSP), and 2) two cascade impactors (Sierra Instruments, model 236) attached to the Hi-Vol samplers to fractionate atmospheric suspended particles in six ranges of size: > 7.2 μm, 3.0–7.2 μm, 1.5–3.0 μm, 0.95–1.5 μm, 0.49–0.95 μm and < 0.49 μm of diameter. The sum of the atmospheric suspended particles collected on the first and last three ranges of size are denominated here as coarse (> 1.5 μm) and fine (< 1.5 μm) particles, respectively. Sample and blank filters (one per sampling period) were

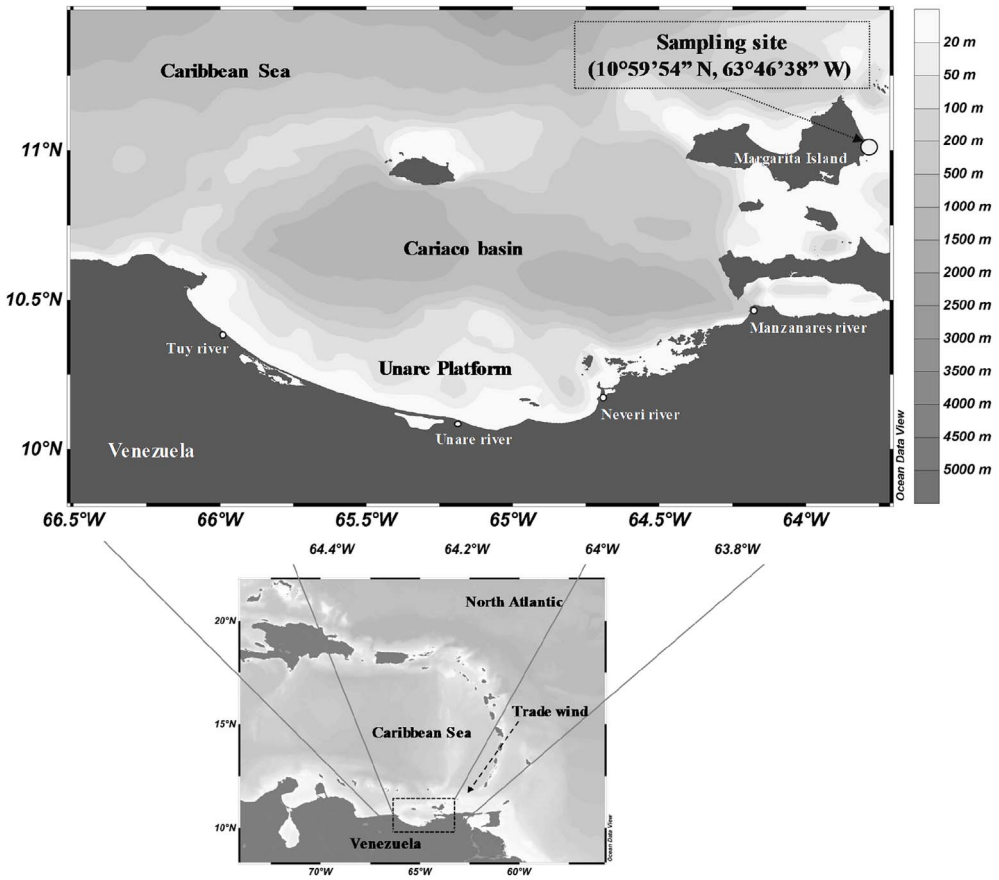

Fig. 1. Area of study. In the top figure is indicated the sampling site (white circle) and the Cariaco basin location. In the bottom figure, the black arrow indicates the predominant trade wind direction.

stored in combusted aluminum foils and preserved at -2 °C until analysis. Individual sample information as well as total and stage cascade impactor suspended particle concentrations are provided in the supplementary material.

2.1.2. Rainfall samples and meteorological data

Duplicate samples of wet deposition were collected by two independent wet deposition samplers. Samples were stored in pre-cleaned (HCl 10% and Milli-Q water) 10 ml polycarbonate bottles and preserved with chloroform at 4 °C at the end of the rainfall events. Milli-Q water blanks were stored and preserved as described above for rainfall samples. Wind velocity and direction were measured from a Campbell Scientific meteorological station.

2.2. Sampling processing and chemical analysis

To extract soluble ions (cations: NH_4^+, Ca^{2+}, Na^+ and K^+; anions: NO_3^-, NO_2^-, SO_4^{2-}, and Cl^-) from TSP samples, we cut the sample filters in six equivalent sections and used three of these to carry out individual extractions. For samples of size-fractionated suspended particles, we used a half of the filters to achieve detectable soluble ions concentration by ion chromatography. We did ultrasound extractions (ultrasonic Bandelin Sonorex model RK106S) of the filters sections with 30 ml of Milli-Q water for 30 min. One half of the final solution was frozen at −20 °C for subsequent DON analysis and the other half was preserved with chloroform at 4 °C until analysis. A similar extraction process was conducted for the blank filters.

Soluble ions concentrations were measured by ion chromatography (Dionex DX 500). For anions, we used a Dionex AS4A anions exchange column, an ASRS-Ultra II suppressor and sodium hydroxyl (11 mM) as eluent. For cations, we used a Dionex CS12A cations exchange column, a CSRS-Ultra II suppressor and sulfuric acid (11 mM) as eluent. Finally, ion concentrations were corrected by subtracting the values found in the blank filters. We obtained residuals lower than 5% for all ions (calculated as the difference between the known ion concentration and that predicted from the linear regression and multiplied by 100).

2.3. UV digestions of DON

We used a generic UV digestion systems consisting of: 1) A 1200-W mercury vapor lamp (Jeilight Co. Inc., model UVC 1501) surrounded by a semi-fixed aluminum carousel with a total capacity of 12 quartz vials; and 2) a ventilation system that keeps the internal temperature below 40 °C during the run time. The linearity of the method ranges between 2.8×10^{-2} and 0.6 mg N l^{-1} and the standard deviation is1.7×10^{-2} mg N l^{-1}.

To convert DON to DIN ($NH_4^+ + NO_3^- + NO_2^-$), we filled pre-combusted quartz tubes with 15 ml of samples (or blanks) and 200 µl 30% hydrogen peroxide (H_2O_2, Sigma Aldrich, ACS grade) as indicated in Bronk et al. (2000). Quartz tubes were hermetically closed with Teflon-lined silicon septa and aluminum crimp tops. Samples were then digested for 90 min to guaranty an optimum oxidation of the DON (≥95%). This time of optimum oxidation was previously established by digesting solutions of known DON concentration (0.28 mg-N l^{-1}, glycine, urea, and a mixed of amino-acids (glycine, trionine, serine and arginine); Sigma Aldrich, ACS grade, ≥ 99%) for different periods of time (30–180 min, data not shown). Oxidized samples were stored in pre-cleaned (HCl 10% and Milli-Q water) 30 ml polycarbonate bottles and preserved with chloroform at 4 °C until analysis. Finally, DON concentration was calculated by the difference between DIN measured by ion chromatography post and prior UV digestion.

2.4. Back trajectory analysis

Back trajectories were performed by the Hybrid Single-Particle Lagrangian Integrated Trajectory model (HYSPLIT, http://www.hysplit.uhu.es/hysplitweb08/HYSPLIT_traj.php). Daily back trajectories were performed for 48 h at 250 m height to represent the airflows at the surface and to track the origin of the air masses for each day of the sampling periods.

2.5. Volume-weighted mean

Ion concentration values in wet deposition samples are inversely proportional to the volume of the rainfall events (Hendry et al., 1984; Lindberg, 1982). To remove this dilution effect, we computed the volume-weighted mean (VWM) of the ions using equation (1). Where C_i is the concentration of the ions (e.g., NO_3^-, NH_4^+) in wet deposition samples and V_i is the volume of the rainfall events.

$$VWM = \sum_i^n \frac{(C_i V_i)}{V_i} \quad (1)$$

2.6. Non sea salt ion concentration (nss-ion)

Mean concentration of non-sea salt component of Ca^{2+} (nss-Ca^{2+}), SO_4^{2-} (nss-SO_4^{2-}) and K^+(nss-K^+) was calculated by equation (2):

$$[X]_{nss} = [X]_{sample} - \left([Na^+]_{sample} * \frac{[X]_{seawater}}{[Na^+]_{seawater}} \right) \quad (2)$$

where $[X]_{nss}$ is the concentration of the non-sea salt component of the ions. $[X]_{sample}$and $[X]_{seawater}$are the ion concentration in the sample and seawater, respectively. $[Na^+]_{sample}$ and $[Na^+]_{seawater}$refer to the corresponding Na^+ concentration in the sample and seawater. We used as reference the sea salt ion concentration reported in Finlayson Pitts and Pitts (2000).

2.7. Atmospheric deposition in the Cariaco basin

TDN atmospheric deposition to the basin was estimated by only using wet and particle deposition of TDN because N gaseous species were not measured here. Wet deposition (W_d, in ton-N year^{-1}) was calculated by:

$$W_d = \sum_i^n V_p [TDN]_i A_{basin} F_w \quad (3)$$

where [TDN] is the VWM-TDN (VWM-DON + VWM-DIN) in units of mg-N l^{-1} (section 2.5). V_p is the median precipitation (mm) for the wet (330.2 mm) and dry (165.2 mm) seasons, respectively. Seasonal V_p was calculated from historical precipitation data (1921–2006) measured at the northeast of the Venezuelan coast and in the Margarita Island. A_{basin} is the area of the Cariaco basin (11.2×10^9 m^2) and F_w (1×10^{-9} ton-N mg-N^{-1}) is the N weight conversion factor.

Particle deposition of TDN (D_p, in ton-N year^{-1}) was calculated as follows:

$$D_p = \sum_i^n k_i [TDN]_i A_{basin} F_d \quad (4)$$

where [TDN] is the concentration of TDN (DON + DIN) in size-fractionated suspended particles in units of µg-N m^{-3}and k_i is the velocity deposition rate (cm s^{-1}) assigned to each range of particle size. F_d is the units conversion factor (3.2×10^{-7} [m cm^{-1}] [s year^{-1}] [ton-N µg-N^{-1}]). We derived k_i by the water tunnel model (Finlayson-Pitts and Pitts-Jr, 2000) and found k_i values (0.01–2.0 cm s^{-1}) similar to those reported in the literature (0.02–2.0 cm s^{-1} from Baker et al., 2010; Farmer and Cohen, 2008). We finally assumed that W_d and D_p took place homogeneously over the whole basin.

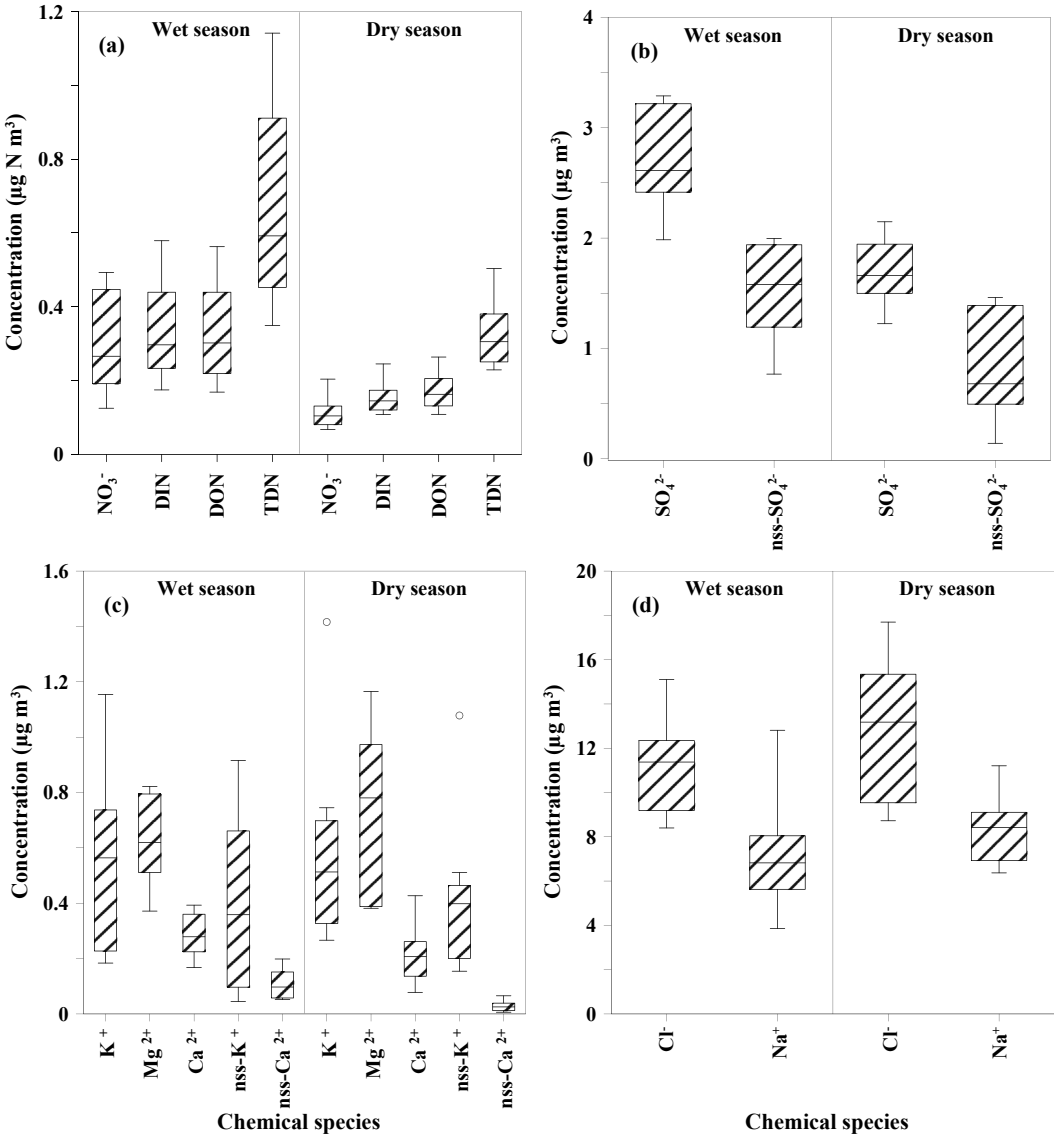

Fig. 2. Concentration of the chemical species in total suspended particle: (a) Dissolved nitrogen species, (b) total SO_4^{2-} and nss-SO_4^{2-}, (c) K^+, Mg^{2+}, Ca^{2+}, nss-K^+ and nss-Ca^{2+} and (d) Cl^- and Na^+. Upper and lower limits of the boxes are the maximum and minimum values, respectively. The entire box describes the likely range of variation (interquartile range-IQR) while its internal horizontal-line is the median. The circles are the outliers (3 × IQR).

3. Results and discussion

3.1. Concentration of ions in atmospheric suspended particles

3.1.1. Total suspended particles

Mean concentrations (± standard deviation) of total suspended particulate DIN and DON were 0.31 ± 0.11 µg-N m^{-3} and 0.32 ± 0.12 µg-N m^{-3} for the wet season, and 0.15 ± 0.04 µg-N m^{-3} and 0.17 ± 0.04 µg-N m^{-3} for the dry season, respectively (Fig. 2). DON accounted on average of half of the total suspended particulate TDN (50 ± 6%, Fig. 2) while NO_3^- was the predominant component of DIN in TSP (86 ± 4%, Fig. 2). DIN and DON concentrations were found to be between the range of those reported in coastal and open ocean regions (range: 0.02–1.22 µg-N m^{-3}; Chen and Chen, 2010; Lesworth et al., 2010; Mace et al., 2003a,b; Miyazaki et al., 2011; Nakamura et al., 2006; Spokes et al., 2000; Violaki and Mihalopoulos, 2010; Violaki et al., 2010; Zamora et al., 2011).

The concentrations of other ions in TSP (Ca^{2+}, Mg^{2+}, SO_4^{2-}, Na^+ and Cl^-, Fig. 2) were also within the range reported in open ocean regions (Heintzenberg et al., 2000; Huang et al., 2001; Savoie et al., 2002) except for K^+ which was on average two times higher (oceanic K^+ = 0.1–0.6 µg m^{-3} from Savoie and Prospero, 1980 and K^+ = 0.18–1.62 µg m^{-3} from this study). Mean nss-concentrations of 0.17 ± 0.12 µg m^{-3}-[nss-Ca^{2+}], 1.42 ± 0.47 µg m^{-3}-[nss-SO_4^{2-}], and 0.50 ± 0.37 µg m^{-3}-[nss-K^+], were found for the wet season. For the dry season, these values were 0.02 ± 0.02 µg m^{-3}-[nss-Ca^{2+}], 0.39 ± 0.35 µg m^{-3}-[nss-SO_4^{2-}], and 0.37 ± 0.26 µg m^{-3}-[nss-K^+]. Overall, mean concentrations of DON, DIN, nss-SO_4^{2-} and nss-Ca^{2+} were between two to nine times higher during the wet season. We did not observe a seasonal pattern for nss-K^+ (Fig. 2).

3.1.2. Size-fractionated suspended particles

3.1.2.1. Fine particles. Average concentrations (± standard deviation) of fine particulate DIN and DON were twice as large during the wet season, with values of 0.06 ± 0.03 µg-N m^{-3} and 0.10 ± 0.05 µg-N m^{-3} (wet season), and 0.03 ± 0.02 µg-N m^{-3} and 0.04 ± 0.01 µg-N m^{-3} (dry season), respectively (Fig. 3 and Table 1). Similarly, mean concentrations of nss-SO_4^{2-}, nss-K^+, nss-Ca^{2+} and Na^+ were between two to six times higher for the same season (Fig. 3 and Table 1). For the whole sampling period, the relative contribution of DIN and DON to

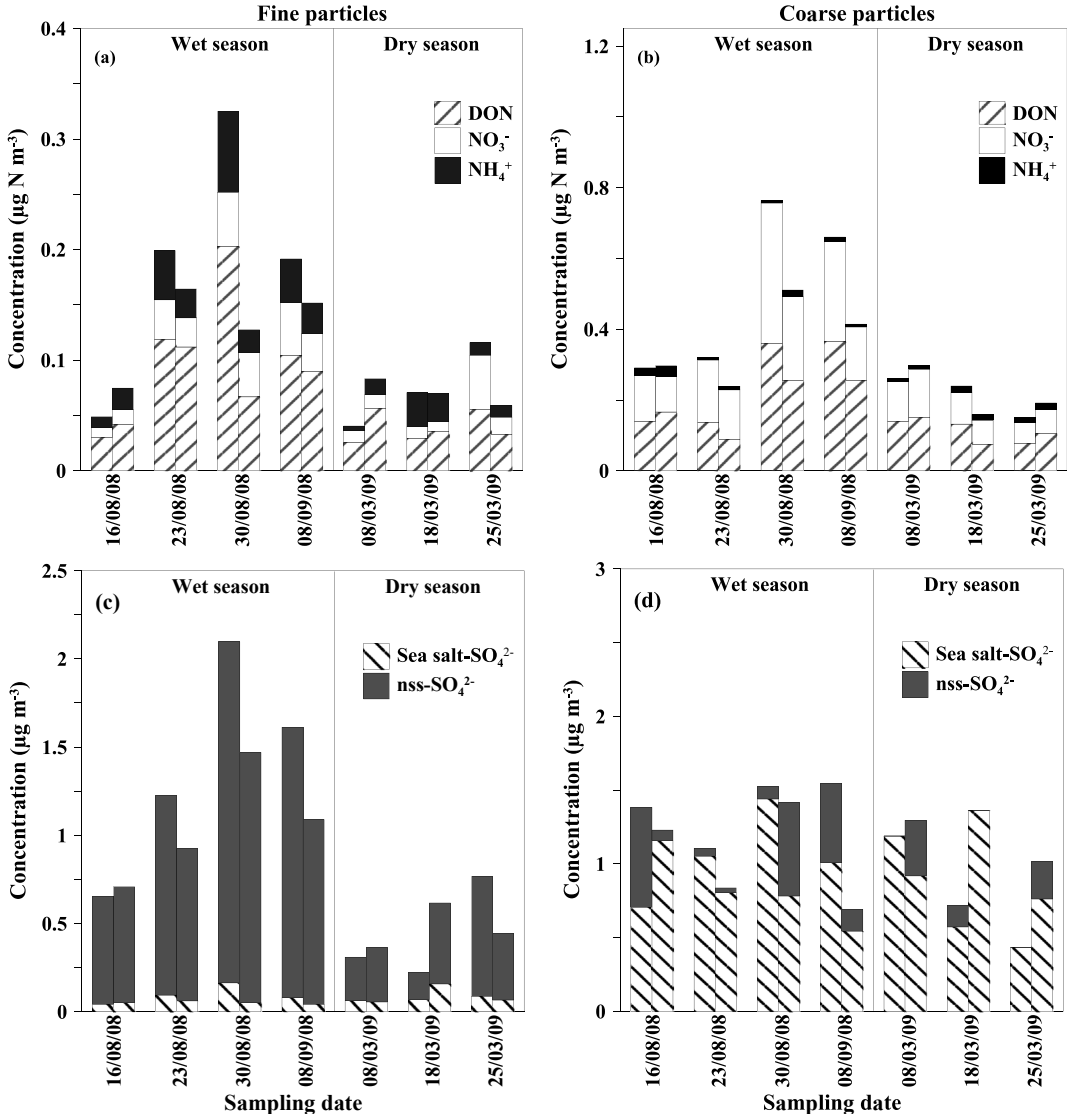

Fig. 3. Concentration of: (a–b) dissolved nitrogen species and (c–d) sea salt SO_4^{2-} and nss-SO_4^{2-} in fine and coarse particles, respectively. The dates below the bars refer to the starting date of the sampling period (which ranged between 5 and 7 continuous days).The two bars at each date represent duplicate samples per sampling period. The differences between the two bars are derived from the spatial concentration variability.

fine particulate TDN was on average 40 ± 4% and 60 ± 4%, respectively. NH_4^+ and NO_3^- accounted for about 58 ± 11% and 42 ± 12% in fine particulate DIN, correspondingly (Table 1).

Fine particles contributed less than 30% of the DON, DIN, nss-$K^+$and Na^+ present in TSP. In contrast, they accounted for about 75 ± 29%, 59 ± 10% and 52 ± 25% of the nss-SO_4^{2-}, NH_4^+, and nss-Ca^{2+} in TSP, respectively (Fig. 3 and Table 1).

3.1.2.2. Coarse particles. Mean concentrations of coarse particulate DIN and DON were twice as large during the wet season such as observed for fine particulate DIN and DON (Fig. 3 and Table 1). On average, coarse particulate DIN and DON have equal contribution to the coarse particulate TDN, while NH_4^+ and NO_3^- accounted for about 7 ± 4% and 93 ± 4% of the coarse particulate DIN, respectively (Table 1).

Coarse particles contributed more than 70% of the DON, DIN (93% as NO_3^-), nss-K^+, Na^+, and Cl^- in TSP. For nss-SO_4^{2-}, NH_4^+, and nss-Ca^{2+} ions, the coarse fraction contribution was smaller (25 ± 29%, 41 ± 10% and 48 ± 25% of TSP, respectively, Fig. 3 and Table 1).

3.1.3. Seasonal variability of DIN and DON sources in atmospheric suspended particles

3.1.3.1. Meteorological data and back trajectories. The mean wind velocity was 3.2 ± 0.4 m s^{-1} and 3.3 ± 0.3 m s^{-1} for the wet and dry seasons, respectively (Figs. 4 and 5). Wind direction indicates a continental influence twice greater for the wet season (e.g., 35 ± 12% of the wind range between 135° and 330° for the wet season, Figs. 4 and 5). In addition, back trajectories show that most of the air masses originated from the continent during the periods with largest content of TDN and nss-SO_4^{2-} in suspended particles (Figs. 2, 3 and 6, e.g., the last three sampling periods of the wet season). In contrast, for the dry season, most of the air masses derived from the Atlantic Ocean (Fig. 7). The later results suggest that continental air masses led to increasing the concentration of chemical species in atmospheric suspended particles during the wet season (e.g., DIN, DON, nss-Ca_2^+ and nss-SO_4^{2-}, Figs. 2 and 3).

3.1.3.2. Chemical tracers of DON and DIN in TSP. We did not find significant correlations between dissolved nitrogen species (DON and DIN) and nss-Ca^{2+}, and nss-K^+ in TSP (R ranged between 0.08 and 0.21, $p > 0.05$, Table 2, Pearson test). We thus discarded continental

Table 1
Concentration (μg m^{-3}) of chemical species in fine and coarse particles during the wet and dry seasons.

Chemical species	Wet season				Dry season				[c]Statis par.	Contribution to TSP
Fine particles (< 1.5 μm)										
	Mean (n = 8)	stdv	[a]Min	[b]Max	Mean (n = 6)	stdv	Min	Max	*P* (n = 14)	(Mean ± std) (n = 14)
DIN	0.06	0.03	0.02	0.12	0.03	0.02	0.01	0.06	0.001	27.6 ± 10.0
DON	0.10	0.05	0.03	0.20	0.04	0.01	0.03	0.06	0.004	29.5 ± 12.4
NO_3^-	0.03	0.01	0.01	0.05	0.01	0.00	0.01	0.02	0.002	16.6 ± 9.4
NH_4^+	0.03	0.02	0.01	0.07	0.02	0.01	< 0.01	0.03	0.174	58.6 ± 10.0
nss-SO_4^{2-}	1.15	0.46	0.61	1.93	0.37	0.18	0.15	0.68	0.001	74.7 ± 29.0
SO_4^{2-}	1.22	0.49	0.65	2.10	0.41	0.16	0.22	0.68	0.002	35.1 ± 20.2
nss-K^+	0.13	0.13	0.04	0.44	0.06	0.02	0.04	0.10	0.035	33.0 ± 15.0
nss-Ca^{2+}	0.06	0.03	0.03	0.10	0.01	0.01	0.01	0.03	0.002	51.7 ± 24.6
K^+	0.15	0.14	0.05	0.44	0.07	0.03	0.05	0.12	0.036	21.9 ± 11.6
Ca^{2+}	0.07	0.03	0.04	0.11	0.02	0.01	0.02	0.04	0.007	15.8 ± 10.6
Na^+	1.33	0.58	0.76	2.21	0.45	0.18	0.24	0.77	0.043	10.8 ± 8.6
Cl-	0.54	0.20	0.30	0.83	0.36	0.04	0.32	0.42	0.973	4.1 ± 2.4
Mg^{2+}	0.04	0.02	0.02	0.08	0.04	0.02	0.03	0.08	0.803	6.4 ± 2.6
Coarse particles (> 1.5 μm)										
DIN	0.21	0.10	0.13	0.40	0.10	0.03	0.07	0.15	0.028	72.4 ± 10.0
DON	0.22	0.10	0.09	0.36	0.11	0.03	0.07	0.15	0.022	70.5 ± 12.4
NO_3^-	0.20	0.10	0.10	0.40	0.09	0.03	0.06	0.14	0.013	83.4 ± 9.4
NH_4^+	0.01	0.01	0.01	0.03	0.01	0.00	0.01	0.02	0.914	41.4 ± 10.0
nss-SO_4^{2-}	0.28	0.28	0.03	0.68	0.35	0.44	0.00	1.02	0.110	25.3 ± 29.0
SO_4^{2-}	1.22	0.32	0.69	1.55	1.00	0.36	0.43	1.36	0.797	64.9 ± 20.2
nss-K^+	0.17	0.10	0.04	0.30	0.24	0.10	0.12	0.34	0.224	67.0 ± 15.0
nss-Ca^{2+}	0.07	0.03	0.03	0.10	0.01	0.01	0.00	0.02	0.000	48.3 ± 24.6
K^+	0.32	0.13	0.16	0.50	0.43	0.13	0.22	0.61	0.164	78.1 ± 11.6
Ca^{2+}	0.26	0.09	0.19	0.46	0.17	0.06	0.10	0.24	0.115	84.2 ± 10.6
Na^+	6.35	1.89	3.47	9.13	7.34	2.14	4.07	10.4	0.126	89.2 ± 8.6
Cl-	10.2	3.01	4.70	14.2	27.5	13.8	13.4	43.8	0.585	95.9 ± 2.4
Mg^{2+}	0.56	0.18	0.34	0.75	0.65	0.25	0.34	0.95	0.372	93.6 ± 2.6

[a]Minimum; [b]Maximum; [c]Statistical parameter *p*. A two way-ANOVA was performed to compute significance differences in ions concentrations between seasons. The difference is significant at the 0.05 level ($p < 0.05$).

dust and biomass burning as DIN and DON sources in TSP (Andreae, 1983; Mace et al., 2003b). In contrast, we found linear correlations between: DIN vs. DON ($R^2 = 0.91$, Fig. 8a), DON vs. SO_4^{2-} ($R^2 = 0.72$, Fig. 8b), and DIN vs. SO_4^{2-} ($R^2 = 0.78$, Fig. 8c), which indicates a common anthropogenic source for DON, DIN and SO_4^{2-} (e.g., SO_2 and NO_x from fossil fuel combustion, Finlayson-Pitts and Pitts-Jr, 2000; Seinfeld and Pandis, 1998). Although, it cannot be ruled out that oxidation of ocean dimethyl sulphide (DMS) could have also provided a significant nss-SO_4^{-2} source large enough to react with nitrogen oxidation products (organic and inorganic) from natural and anthropogenic origins (e.g., Stark et al., 2007).

3.1.3.3. DIN and DON in fine particles. Fine particulate TDN represents less than 30% of the TSP TDN; however, their NO_3^- and nss-SO_4^{2-}composition could reflect cluster nucleation derived from trace gases secondary reactions (e.g., NO_x, SO_2 and DMS, Atkinson and Arey, 2003; Bates et al., 1992; Heintzenberg et al., 2000; Stark et al., 2007). We found that fine particulate DON, DIN, and nss-SO_4^{2-} increased between two to four times for the season with largest continental influences (e.g., last three sampling periods of the wet season, Table 1 and Fig. 3). In addition, we found linear correlations between fine particles: NO_3^- vs. nss-SO_4^{2-} ($R^2 = 0.93$, Fig. 9a), DON vs. nss-SO_4^{2-} ($R^2 = 0.71$, Fig. 9b), DON vs. NO_3^- ($R^2 = 0.68$, Fig. 9c), and DON vs. DIN ($R^2 = 0.93$, Fig. 9d), which confirms the hypothesis that fine particles DON, DIN and nss-SO_4^{2-} increased during the wet season because of the oxidation of continent-derived NO_x and SO_2. We discarded NO_x and SO_2 emission from shipping because this activity is not significant in the studied region. The largest port of the island is the Guamache Port where ferries and cruises land. This is a small port located on the south west part of the island with no effect on our sampling site, in view of the air masses direction during our study (Figs. 4–7).

We also found that fine particulate DON concentrations were significantly correlated with fine particulate DIN ($R^2 = 0.93$, Fig. 9d) and fine particulate NH_4^+ ($R = 0.872$, $p > 0.05$, Table 2, Pearson test). This last finding indicates there was a secondary source of DON linked to NH_4^+ (e.g., reduced DON from the oxidation of reduced nitrogen and VOCs; Altieri et al., 2012 and references therein; Bones et al., 2010; Updyke et al., 2012), and supports the hypothesis that formation/deposition pathways of NH_4^+ and reduced DON are related (Ito et al., 2014 and references therein).

Finally, the positive correlation only found between fine particulate DON, DIN and nss-SO_4^{2-} (Fig. 9 and Table 2), indicates that SO_4^{2-}derived from the oxidation of SO_2 and DMS could have formed fine particles DIN and DON through heterogeneous reactions with N trace gases (Seinfeld and Pandis, 1998).

3.1.3.4. DIN and DON in coarse particles. As mentioned above, coarse particulate TDN contains about 70% of TDN (for DON and DIN) in TSP (Fig. 3 and Table 1). From the possible particle TDN sources, we ruled out continental dust due to weak correlations between DON, DIN and nss-Ca^{2+} in coarse particulate and TSP (Table 2, e.g., Mace et al., 2003b). We therefore propose two possible mechanisms that justify this large proportion of TDN in the coarse particles: 1) DIN (e.g., as nitric acid: HNO_3) and DON can be quickly absorbed-dissolved onto-into the coarse particles after being formed by secondary reactions (e.g., Cornell et al., 2001; Violaki et al., 2015; Violaki and Mihalopoulos, 2010; Zamora et al., 2011), and 2) the surface ocean can also release a fraction of coarse particulate DON (e.g., amines and alkyl nitrates (C_1-C_3), Dahl et al., 2007; Mace et al., 2003a; Miyazaki et al., 2011). However, we think this second mechanism might be minor because the strong positive correlation between coarse particulate NO_3^- and DON indicates a common source ($R = 0.89$, Table 2, Pearson test; e.g., oxidation of NO_x). The latest finally suggests that coarse particulate

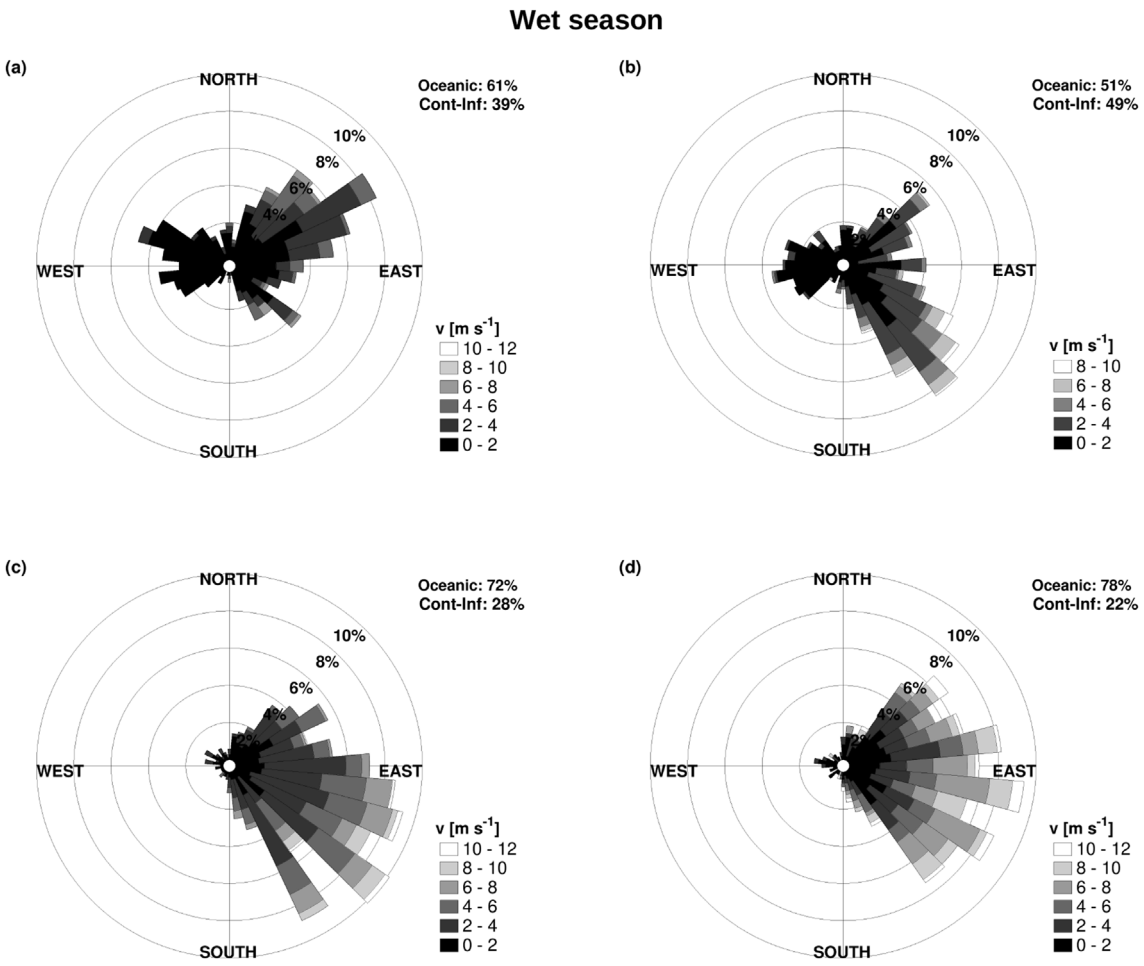

Fig. 4. Wind roses for the wet season sampling periods. The bars indicate the frequency (in %) of the wind for a given range of direction (in degrees), while the gray scale inside the bars describe the wind velocity range (m s^{-1}). North, East, South and West are the cardinal directions that correspond to 0°/360°, 90°, 180° and 270°, respectively. Figures (a), (b), (c) and (d) are the first, second, third, and fourth sampling periods, respectively. The terms Oceanic and Cont-inf refer to the wind derived (in %) from the Atlantic Ocean (330°–135°) and with potential continental influence (135°–330°), respectively.

DON should be mainly encompassed of alkyl nitrates.

3.2. Concentration of ions in wet deposition

3.2.1. Chemical composition

Mean concentrations (± standard deviation) of DON and DIN in wet deposition samples were 0.22 ± 0.18 mg-N l^{-1} and 0.13 ± 0.11 mg-N $l^{-1}$for the wet season, and 0.33 ± 0.44 mg-N l^{-1} and 0.17 ± 0.01 mg-N l^{-1} for the dry season, respectively (Table 3). DON and DIN values reported here are in the same order of magnitude that those reported for other Venezuelan sites (0.34–1.00 mg-N l^{-1}, Morales et al., 2001; Pacheco et al., 2004). In general, concentrations of other ions were at least double during the dry season (i.e., SO_4^{2-}, Ca^{2+} and K^+, Table 3).

Concentrations of DON and DIN were not significantly different between seasons ($p > 0.05$, n = 16, two way-ANOVA test), whereas nss-SO_4^{2-} was 2 times larger during the dry season (Table 3). We found significant negative correlations between precipitation and DON, DIN, and nss-SO_4^- concentrations (R ranged between −0.62 and −0.43, $p < 0.05$, Table 4, Pearson test). We, therefore, calculated and used the volume weight mean concentration (VWM) to assess TDN wet deposition as described in sections 2.5 and 2.7. We finally found that VWM-DON accounted for about 60 ± 1.3% of VWM-TDN, whereas VWM-NH_4^+ had the largest contribution to VWM-DIN (61 ± 20%, Table 3).

3.2.2. Potential sources of DON and DIN in wet deposition

Unlike for atmospheric particles, we found modest correlations between DON and DIN (R = 0.64, $p < 0.05$, Table 4, Pearson test). This difference can be attributed to the follow factors that affect the chemical composition of the rainfall events: 1) Volume and intensity of the events, and 2) the physicochemical properties of particles and gases scavenged (e.g., polarity and velocity deposition rate; Hendry et al., 1984; Lindberg, 1982). For instance, the largest contribution of VWM-NH_4^+ (61 ± 20%) to DIN wet deposition should be linked to the sources and removal rate of nitrogen species driving the content of NH_4^+ and NO_3^- available for scavenging.

NH_4^+ in wet deposition is related to ammonia (NH_3) sources (agricultural activities, human waste, and “oceanic emissions”, Altieri et al., 2014; Bouwman et al., 1997; Jickells et al., 2003). NH_3 is highly reactive with sulfuric acid (H_2SO_4) and HNO_3, forming fine particles of ammonium sulfate and ammonium nitrate. These fine particles increase the lifetime of ammonium in the atmosphere and its long-range transport from the continents to the oceans (e.g., Zhao et al., 2015). In contrast, NO_3^- in wet deposition derives from “terrestrial” N gases (such as nitrogen dioxide, nitric acid, and nitrous acid) which are more quickly removed from the atmosphere (Jia et al., 2016 and references therein) and have a major contribution to N gas dry deposition in tropical ecosystems (Trebs et al., 2006). Therefore, above arguments suggest that:1) Long-range transport of fine particles-rich in NH_4^+ (58 ± 11% of fine particulate DIN, Table 1) and oceanic NH_3 emissions might have favored NH_4^+ scavenging rate in comparison to NO_3^-,

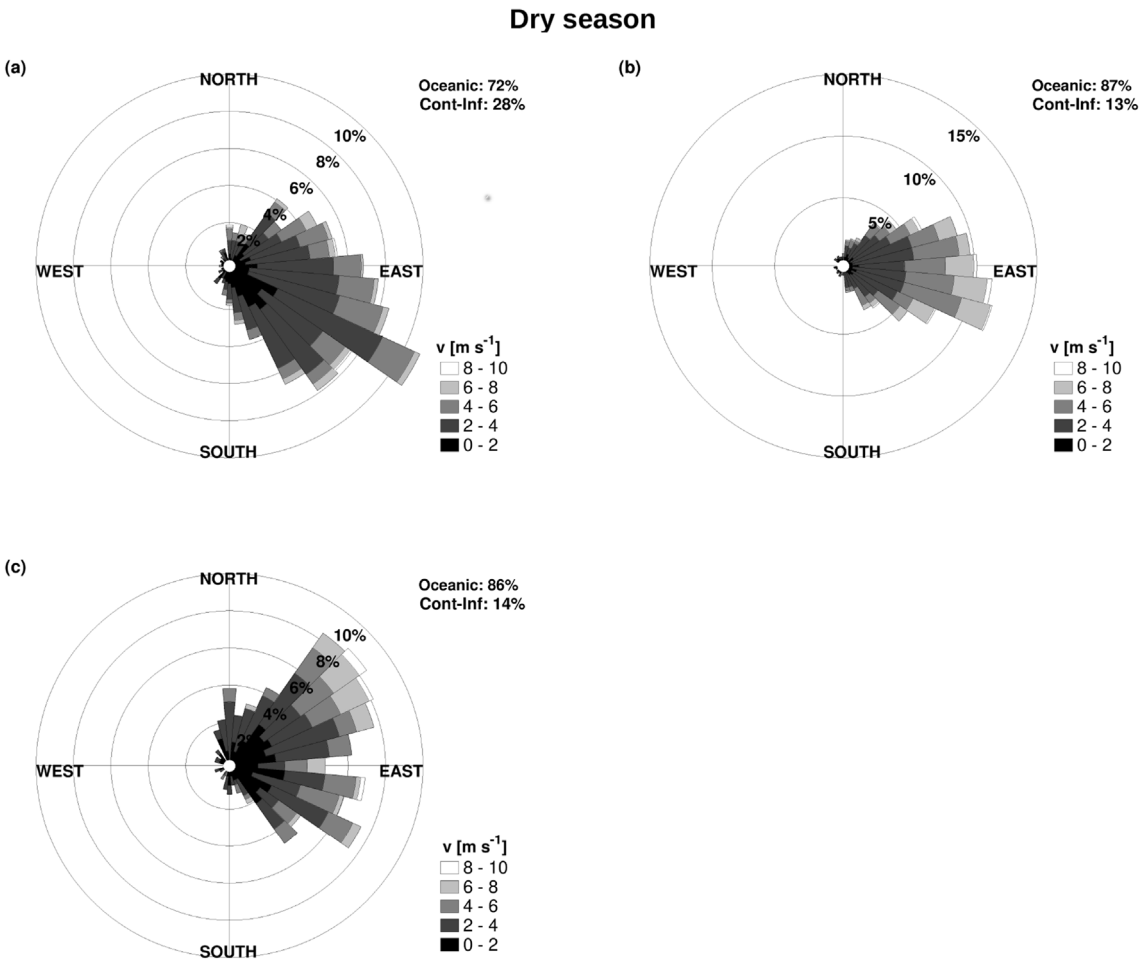

Fig. 5. Wind roses for the dry season sampling periods. The bars indicate the frequency (in %) of the wind for a given range of direction (in degrees), while the gray scale inside the bars describe the wind velocity range (m s^{-1}). North, East, South and West are the cardinal directions that correspond to 0°/360°, 90°, 180° and 270°, respectively. Figures (a), (b) and (c) are the first, second and third sampling periods, respectively. The terms Oceanic and Cont-inf refer to the wind (in %) derived from the Atlantic Ocean (330°–135°) and with potential continental influence (135°–330°), respectively.

which is supported by a good agreement between NH_4^+:DIN ratios in fine particles (0.58 ± 0.12) and wet deposition (0.60 ± 0.20, calculated from the VWM, Table 3); and 2) dry gas deposition of inorganic N may be important in the basin. However, this second hypothesis cannot be corroborated because inorganic nitrogen trace gases were not measured here.

DON in wet deposition derives from scavenging of alkyl nitrates and reduced organic nitrogen species (gas + particles). As discussed above, alkyl nitrates and reduced organic nitrogen are emitted by the ocean (Dahl et al., 2007; Facchini et al., 2008; Miyazaki et al., 2011) and formed by secondary reactions between NO_x, reduced nitrogen species and VOCs (Altieri et al., 2012; Atkinson and Arey, 2003; Bones et al., 2010; Updyke et al., 2012). We found a strong correlation between DON and NH_4^+ ($R = 0{,}871$, $p < 0.05$, Table 4, Pearson test) and a weak one with NO_3^- ($R = 0{,}484$, $p < 0.05$, Table 4, Pearson test) in wet deposition. This indicates that although alkyl nitrates are likely the major component of DON in TSP (70% as coarse particles, section 3.1.3.4), reduced DON linked to NH_4^+ has a significant contribution to DON wet deposition (e.g., Altieri et al., 2012) likely because DON is preferentially scavenged by rainout within the clouds (e.g., dissolution of gases and fine particles into cloud droplets) instead of being washout (e.g., gas + particles scavenged below the cloud, Altieri et al., 2016 and references therein). The latest hypothesis is supported by a good agreement found between NH_4^+:DON ratios in fine particulate (0.40 ± 0.14) and wet deposition (0.41 ± 0.13, calculated from the VWM, Table 3), and is consistent with the argument that pathways of formation, transformation and deposition of NH_4^+ and reduced DON are intimately linked (Altieri et al., 2012, 2016; Ito et al., 2014 and reference therein). Finally, our findings pointed out that reduced DON (gas + particles) should be a significant component of bulk N deposition as suggested in previous works (Altieri et al., 2012; Ito et al., 2014; Matsumoto and Yamato, 2017; Zamora et al., 2011). Unfortunately, this hypothesis cannot be demonstrated because reduced DON was not quantified here.

3.3. TDN atmospheric deposition in the Cariaco basin

Atmospheric deposition of TDN contributes to keep the relative stationary state of N and C cycles in semi-closed marine ecosystems because it supports up to 60% of their new primary productivity (e.g., Mediterrenean Sea, Christodoulaki et al., 2013). For the Cariaco basin, we estimated an annual TDN atmospheric deposition of 3.6×10^3 ton-N $year^{-1}$ (wet + particles) which is within the range loaded by rivers ($0–1.5 \times 10^4$ ton-N $year^{-1}$; Tuy, Unare, Neveri and Manzanares rivers, see Fig. 1; Bustamante et al., 2015). We found this new N replaces between 25 and 40% of the N removed by sediment burial (~1.1×10^4 ton-N $year^{-1}$, Muller-Karger et al., 2010) or by anaerobic N_2 production (~1.5×10^4 ton-N $year^{-1}$, Montes et al., 2013). These results demonstrate that TDN atmospheric deposition plays a key role in the N budget of the basin. This role might be larger because TDN gas dry deposition was not measured in this study and, as mentioned above, could be significant in tropical ecosystems.

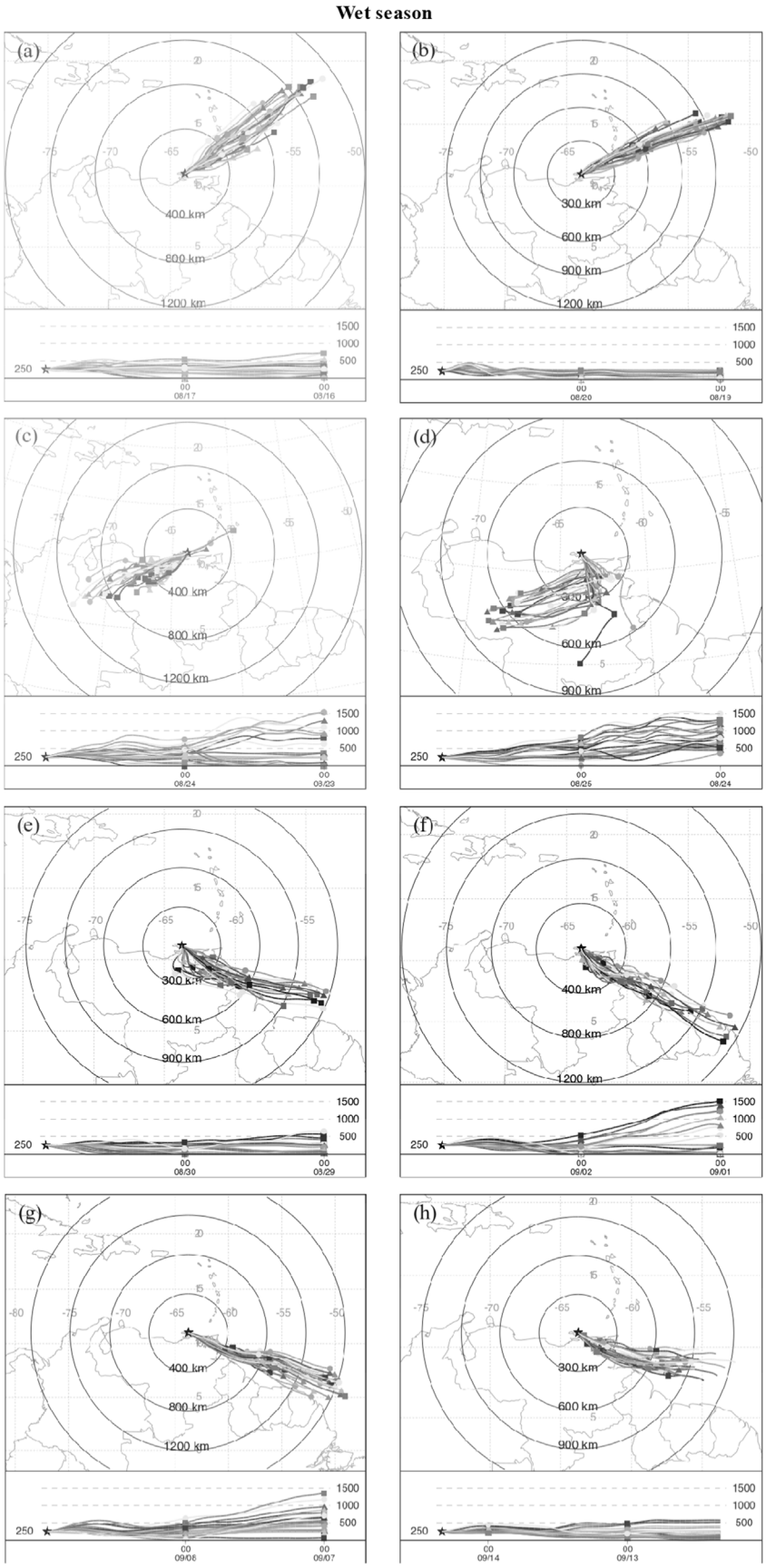

Fig. 6. Selected back trajectories for the wet season sampling periods. The back trajectories were performed for 48 h at 250 m height. Individual figures correspond to: (a) day 3 (08-18-2008) and (b) day 6 (08-21-2008) of the first sampling period, (c) day 3 (08-25-2008) and (d) day 4 (08-26-2008) of the second sampling period, (e) day 2 (08-31-2008) and (f) day 5 (09-03-2008) of the third sampling period, (g) day 2 (09-09-2008) and (h) day 7 (09-14-2008) of the fourth sampling period, respectively. The regressive dates of the air masses are described at the bottom of each run. The complete sequence of the daily back trajectories are described for each sampling period are available in the supplementary material.

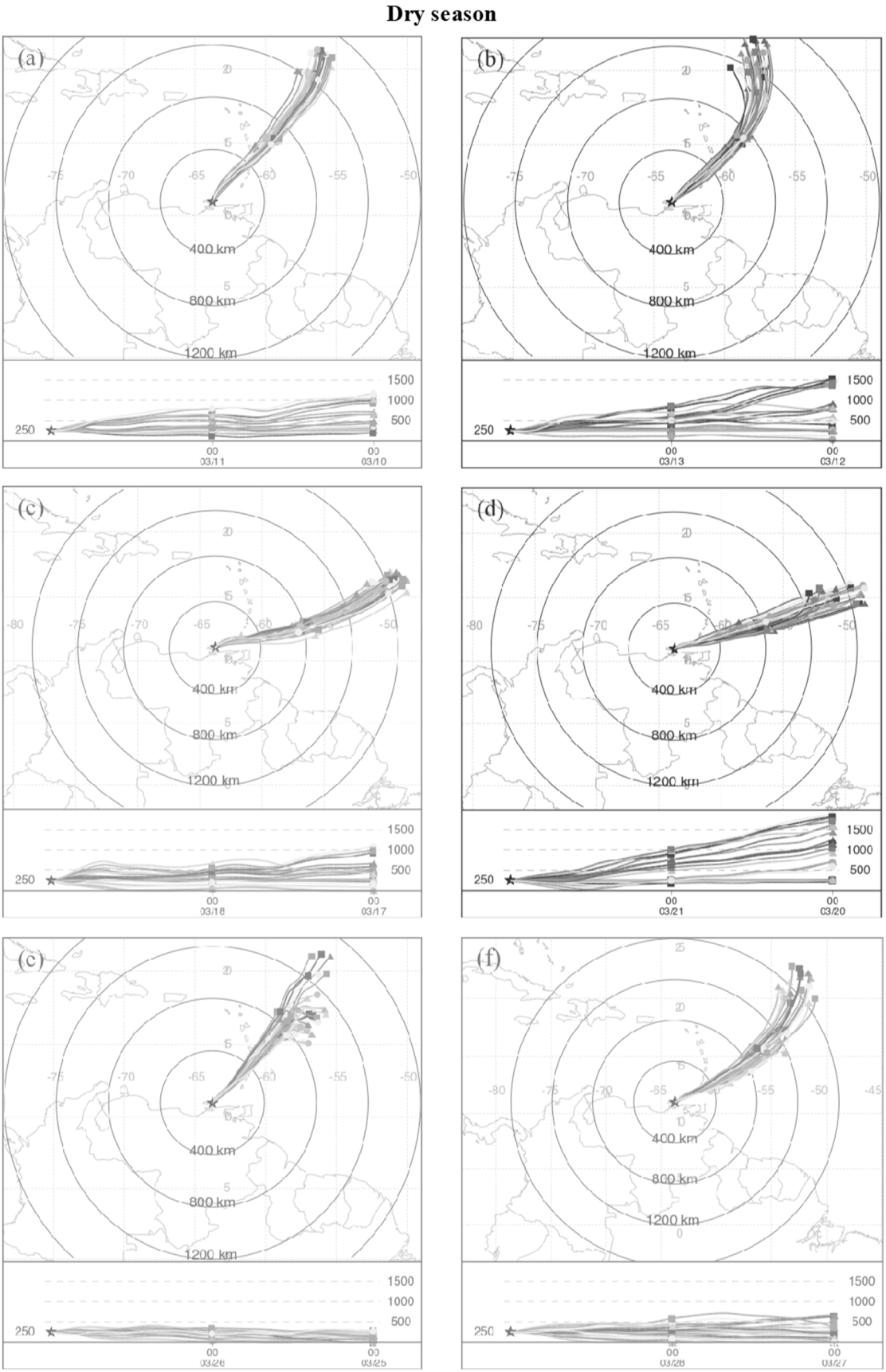

Fig. 7. Selected back trajectories for the dry season sampling periods. The back trajectories were performed for 48 h at 250 m height. Individual figures correspond to: (a) day 2 (03-12-2009) and (b) day 4 (03-14-2009) of the first sampling period, (c) day 2 (03-19-2009) and (d) day 5 (03-22-2009) of the second sampling period, (e) day 3 (03-27-2009) and (f) day 5 (03-29-2009) of the third sampling period, respectively. The regressive dates of the air masses are described at the bottom of each run. The complete sequence of daily back trajectories are described for each sampling period are available in the supplementary material.

Table 2
Binary statistical correlation matrixes computed for the evaluated variables in fine and coarse particles (n = 14) and TSP (n = 26).

Nitrogen species	nss-SO_4^{2-}	nss-K^+	nss-Ca^{2+}	DON	NO_3^-	NH_4^+
Fine particles						
DIN	0.892*	0.326	0.656*	0.959*	–	–
DON	0.836*	0.330	0.659*	–	0.921*	0.872*
Coarse particles						
DIN	−0.203	0.054	0.325	0.888*	–	–
DON	−0.086	0.092	0.346	–	0.888*	−0.273
TSP						
DIN	0.341	0.206	0.103	0.938*	–	–
DON	0.249	0.131	0.083	–	0.908*	0.455*

*The correlation is significant at the 0.05 level.
We performed Pearson correlation coefficient tests using the statistical package SPSS 10.0.

To assess the relevance of TDN atmospheric deposition in the C budget of the basin, we calculated its relative contribution to primary productivity by assuming: a DON bioavailability ranging between 12 and 80% (Bronk, 2002; Bronk et al., 2007; Cape et al., 2011; Peierls and Paerl, 1997; Seitzinger et al., 2002; Wedyan et al., 2007), a C:N ratio of 106:16, and that all DIN is consumed by phytoplankton. We found that TDN atmospheric deposition contributes to a small fraction (0.2–0.3%) of the basin primary productivity (5.8×10^6 ton-C $year^{-1}$, Muller-Karger et al., 2010). However, this small fraction of C ($1.0–1.8 \times 10^4$ ton-C $year^{-1}$) replaces a significant amount of the C (14–25%) removed by sediment burial (7.2×10^4 ton-C $year^{-1}$, Muller-Karger et al., 2010).

Finally, to evaluate how anthropogenic N could be impacting TDN deposited in the basin, we re-calculated TDN particle deposition by excluding atmospheric suspended particles samples with continental influence (selected samples inferred by the performed back trajectories described in Figs. 6 and 7 and supplementary material). We then estimated the continental fraction of this TDN as the difference between TDN particle deposition with (1.7×10^3 ton-N $year^{-1}$) and without (1.1×10^3 ton-N $year^{-1}$) continental influence. We finally assumed that at least 25% of the continental particle deposition (6.0×10^2 ton-N) and wet deposition (1.9×10^3 ton-N) of TDN was anthropogenic (e.g., 45% and 80% of the organic and total nitrogen deposited in the ocean is anthropogenic, respectively, Kanakidou et al., 2012 and Duce et al., 2008). As a result, we estimated that about 30% ($\sim 9.0 \times 10^2$ ton-N $year^{-1}$) of the TDN deposited in the basin could be derived from anthropogenic sources. This estimate should be taken with caution due to the fact that we did not measure TDN deposition in a remote tropical Atlantic ocean site (to account for remote oceanic air masses), but it is a good first approximation that indicates anthropogenic N sources might represent a significant fraction of the nitrogen deposited in the Cariaco basin.

4. Summary and conclusions

We report the first assessment of TDN atmospheric deposition for the Cariaco basin and demonstrated that this new N contributes to maintain the relative stationary states of the C and N cycles in this place.

We estimate that anthropogenic N could be increasing by at least 30% the atmospheric supply of TDN in the basin. Therefore, primary productivity of the basin would increase in the future if the projected industrialization processes in the north east region of Venezuela takes place.

Our results, in conjunction with previous works, suggest that the chemical composition of TDN in wet and particle deposition is not similar because the predominant mechanisms that drive the incorporation of reduced-oxidized DON and DIN (NH_4^+ and NO_3^-) into suspended particles and rainfall differ. They also highlight that scavenging of reduced DON (gas + particles) is a significant component of bulk N deposition in the ocean.

We recommend establishing a long-term atmospheric time series that includes TDN gas dry deposition to improve the current assessment. We also recommend to measure the isotope composition ratios of $^{15}\delta N$ and $^{13}\delta C$ and characterize DON (e.g., reduced organic nitrogen and alkyl nitrates (C_1-C_3)) in wet and atmospheric suspended particles samples. It will allow to separate natural and anthropogenic nitrogen and to better understand the mechanisms responsible of TDN atmospheric composition in the Cariaco basin.

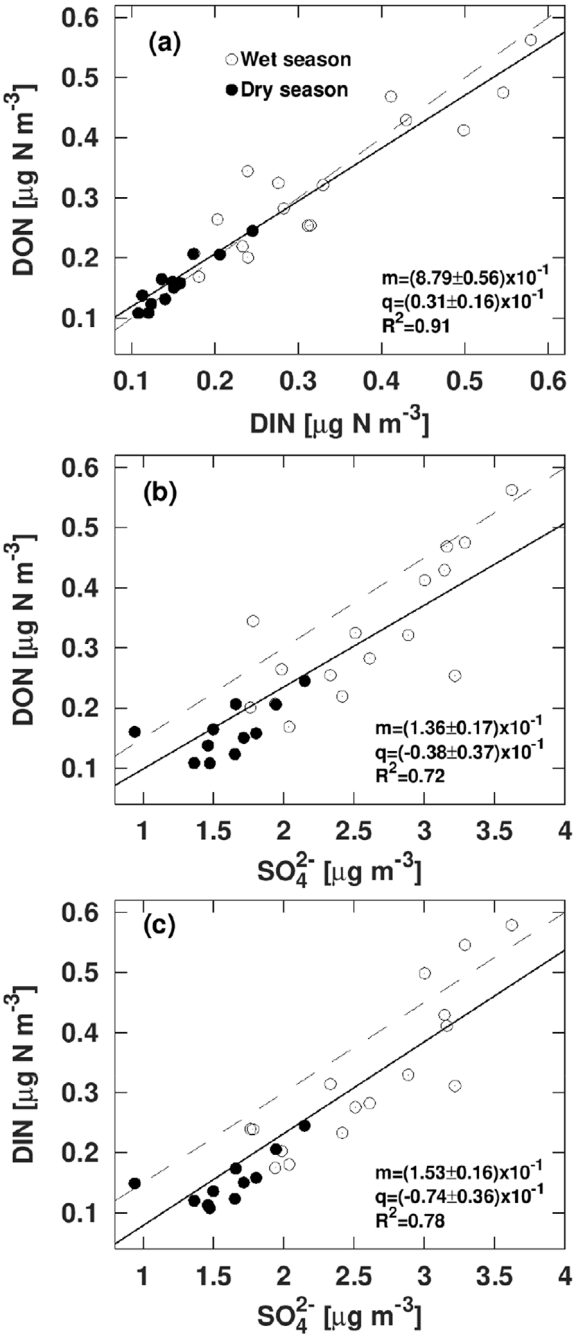

Fig. 8. Linear correlations between: (a) DIN vs. DON, (b) DON vs. total SO_4^{2-} and (c) DIN vs. total SO_4^{2-} in TSP. Black and white circles refer to the dry and wet season, respectively; m and q represent the slope (± error) and intercept (± error) of the linear regression, respectively. Dashed and solid black lines indicate the 1:1 and linear relationships, respectively.

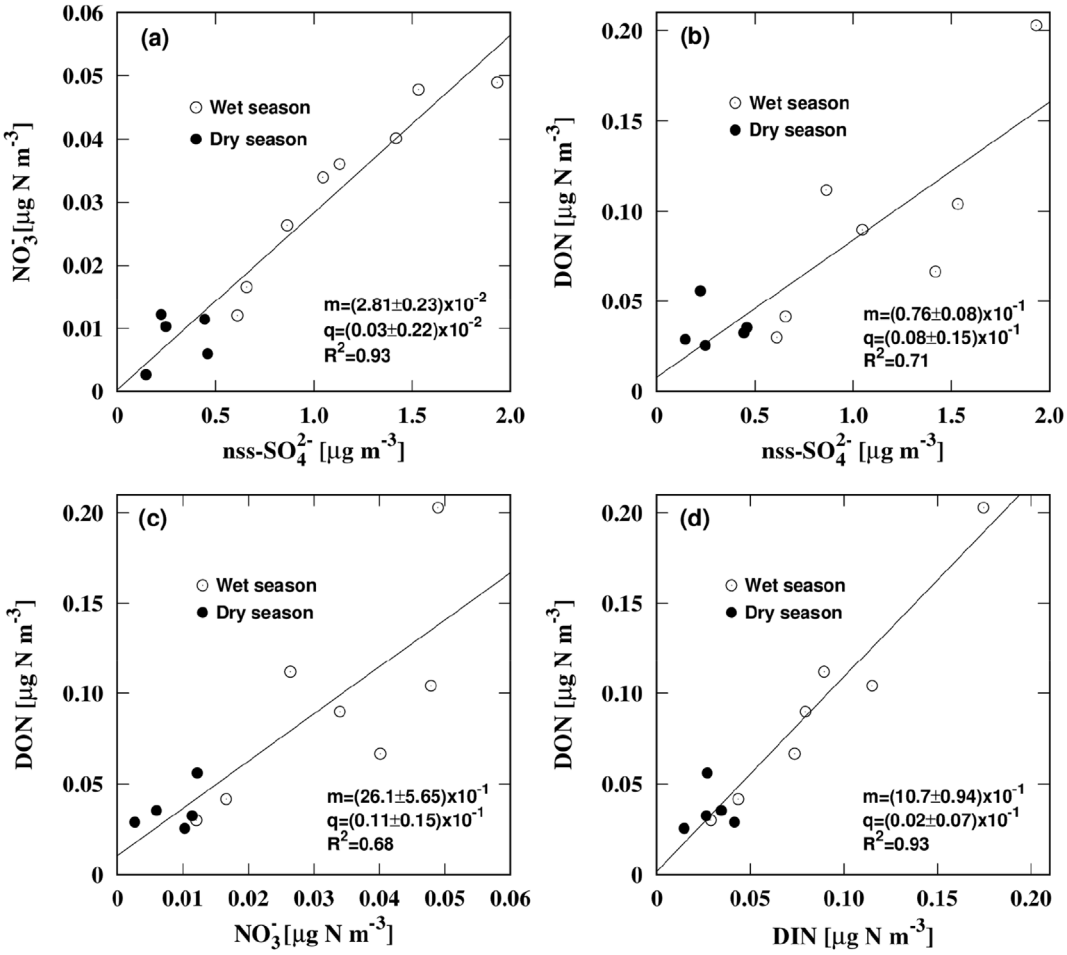

Fig. 9. Linear correlations between fine particles: (a) NO_3^- and nss-SO_4^{2-}, (b) DON and nss-SO_4^{2-}, (c) DON and NO_3^- and (d) DON and DIN. Black and white circles refer to the dry and wet season, respectively; m and q represent the slope (± error) and intercept (± error) of the linear regression, respectively. Black line is the linear relationship.

Acknowledgments

The authors thanks to the Fondo Nacional de Ciencia, Tecnología e Innovación (FONACIT) and to the Instituto Venezolano de Investigaciones Científicas for the graduate school fellowships provided to Rafael Rasse. This work was supported by: 1) FONACIT capacity building award to Rafael Rasse under "Mision Ciencia" program No 200900486 and 2) FONACIT-MCTI No 201200404 "Cariaco basin time series. Climatic and Oceanographic Changes in the Cariaco Basin System". 3) Nnet network: Nitrogen cycling in Latin America: drivers, impacts and vulnerabilities, Inter American Institute for Global Change Research, No CRN 3005. We finally would like to thank Alcides Rojas and Gregorio Maldonado for their collaborations during the field campaigns, to Lieutenant Commander Luis Pivernat, Master Palacios and logistic personnel of the Bolivarian Republic of Venezuelan Navy Pampatar Hidrographic Station for providing their installations to conduct the field campaigns, to Dr. Robert Brewin for his comments, and to the unknown reviewers for their constructive advice and

Table 3
Precipitation, concentration and volume weight mean concentration of nitrogen species and other ions in wet deposition during the dry and wet seasons (mg l^{-1}).

	[b]V_p.	DIN	DON	%DON	NO_3	SO_4^{2-}	[c]nss-S	NH_4^+	Mg^{2+}	Ca^{2+}	K^+	[d]nss-Ca	nss-K^+
Wet season (n = 10)													
Min	3.1	0.07	0.10	51	0.01	0.20	< b.d[e]	0.03	0.06	0.11	0.04	< bl*	0.02
Max	25	0.54	0.73	82	0.17	0.64	0.13	0.37	0.22	0.43	0.21	0.35	0.16
Mean	14	0.13	0.22	59	0.04	0.39	0.07	0.09	0.15	0.28	0.11	0.11	0.06
Stdv	8.5	0.11	0.18	8.6	0.04	0.13	0.03	0.08	0.06	0.13	0.06	0.14	0.05
[a]VWM	–	0.12	0.18	60	0.03	0.44	0.14	0.09	0.15	0.23	0.12	0.08	0.07
Dry season (n = 6)													
Min	1.3	0,11	0.02	6.8	0.03	1.01	0.06	0.04	0.38	0.26	0.16	< b.l	0.01
Max	14.8	0.32	1.29	74	0.16	2.37	0.56	0.16	0.74	0.45	0.42	0.10	0.13
Mean	6.9	0.17	0.33	45	0.09	1.56	0.29	0.08	0.60	0.37	0.29	0.06	0.08
Stdv	5.8	0.10	0.44	25	0.04	0.52	0.26	0.05	0.14	0.07	0.12	0.03	0.07
VWM	–	0.15	0.22	60	0.08	0.93	0.28	0.07	0.37	0.24	0.18	0.06	0.05

[a]VWM is the volume weight mean concentration, while [b]V*p* is the precipitation expressed in mm.
[c,d]non sea salt (nss) sulfate and calcium.
[e]b.d: below the detection limit (~20 nM).
The ions and nitrogen species concentration are expressed in mg l^{-1} and mg-N l^{-1}, respectively.

Table 4
Binary statistical correlation matrix for evaluated parameters in wet deposition (n = 16).

Nitrogen species	V_p	nss-SO_4^{2-}	nss-K^+	nss-Ca^{2+}	DON	DIN	NO_3^-	NH_4^+
[a]*Vp*	–	−0.479*	−0.362	0.424	−0.440*	−0.429*	−0.582*	−0.384
DIN	−0.429*	0.704*	0.329	−0.043	0.643*	–	–	–
DON	−0.440*	0.740*	0.241	−0.252	–	–	0.484*	0.871*

[a]V_p: Precipitation (mm).
**The correlation is significant at the 0.05 level.
We performed Pearson correlation coefficient test (R) using the statistical package SPSS 10.0.

comments that contributed to significantly improve the quality of the manuscript.

Appendix A. Supplementary data

Supplementary data related to this article can be found at http://dx.doi.org/10.1016/j.atmosenv.2018.02.007.

References

Altieri, K.E., Fawcett, S.E., Peters, A.J., Sigman, D.M., Hastings, M.G., 2016. Marine biogenic source of atmospheric organic nitrogen in the subtropical North Atlantic. Proc. Natl. Acad. Sci. Unit. States Am. 113 (4), 925–930.

Altieri, K.E., Hastings, M.G., Peters, A.J., Oleynik, S., Sigman, D.M., 2014. Isotopic evidence for a marine ammonium source in rainwater at Bermuda. Global Biogeochem. Cycles 28 (10), 1066–1080.

Altieri, K.E., Hastings, M.G., Peters, A.J., Sigman, D.M., 2012. Molecular characterization of water soluble organic nitrogen in marine rainwater by ultra-high resolution electrospray ionization mass spectrometry. Atmos. Chem. Phys. 12 (7), 3557–3571.

Andreae, M.O., 1983. Soot carbon and excess fine potassium-long-range transport of combustion-derived aerosols. Science 220, 1148–1151.

Atkinson, R., Arey, J., 2003. Gas-phase tropospheric chemistry of biogenic volatile organic compounds: a review. Atmos. Environ. 37, S197–S219.

Baker, A.R., Lesworth, T., Adams, C., Jickells, T.D., Ganzeveld, L., 2010. Estimation of atmospheric nutrient inputs to the Atlantic Ocean from 50 N to 50 S based on large-scale field sampling: fixed nitrogen and dry deposition of phosphorus. Global Biogeochem. Cycles 24.

Bates, T.S., Calhoun, J.A., Quinn, P.K., 1992. Variations in the methanesulfonate to sulfate molar ratio in submicrometer marine aerosol particles over the South Pacific Ocean. J. Geophys. Res.: Atmos. 97 (D9), 9859–9865.

Bones, D.L., Henricksen, D.K., Mang, S.A., Gonsior, M., Bateman, A.P., Nguyen, T.B., Cooper, W.J., Nizkorodov, S.A., 2010. Appearance of strong absorbers and fluorophores in limonene-O_3 secondary organic aerosol due to NH_4^+-mediated chemical aging over long time scales. J. Geophys. Res.: Atmos. 115 (D5).

Bronk, D.A., 2002. Dynamics of DON. In: Hansell, D.A., Carlsson, G.A. (Eds.), Biogeochemistry of Marine Dissolved Organic Matter. Elsevier Science San Diego, pp. 153–247.

Bronk, D.A., Lomas, M.W., Glibert, P.M., Schukert, K.J., Sanderson, M.P., 2000. Total dissolved nitrogen analysis: comparisons between the persulfate, UV and high temperature oxidation methods. Mar. Chem. 69, 163–178.

Bronk, D.A., See, J.H., Bradley, P., Killberg, L., 2007. DON as a source of bioavailable nitrogen for phytoplankton. Biogeosciences 4, 283–296.

Bouwman, A.F., Lee, D.S., Asman, W.A.H., Dentener, F.J., VanderHoek, K.W., Olivier, J.G.J., 1997. A global high-resolution emission inventory for ammonia. Global Biogeochem. Cycles 11, 561–587.

Bustamante, M.C., Martinelli, L.A., Pérez, T., Rasse, R., Ometto, J.P.H.B., Siqueira Pacheco, F., Machado Lins, S.R., Marquina, S., 2015. Nitrogen management challenges in major watersheds of South America. Environ. Res. Lett. 10, 065007. http://dx.doi.org/10.1088/1748-9326/10/6/065007.

Cape, J.N., Cornell, S.E., Jickells, T.D., Nemitz, E., 2011. Organic nitrogen in the atmosphere - where does it come from? A review of sources and methods. Atmos. Res. 102, 30–48.

Cape, J.N., Anderson, M., Rowland, A.P., Wilson, D., 2005. Organic nitrogen in precipitation across the United Kingdom. Water Air Soil Pollut. Focus 4 (6), 25–35.

Chen, H.Y., Chen, L.D., 2010. Occurrence of water soluble organic nitrogen in aerosols at a coastal area. J. Atmos. Chem. 65, 49–71.

Chen, H.Y., Chen, L.D., Chiang, Z.Y., Hung, C.C., Lin, F.J., Chou, W.C., Gong, G.C., Wen, L.S., 2010. Size fractionation and molecular composition of water-soluble inorganic and organic nitrogen in aerosols of a coastal environment. J. Geophys. Res.: Atmos. 115 (D22).

Chen, Y.X., Chen, H.Y., Wang, W., Yeh, J.X., Chou, W.C., Gong, G.C., Tsai, F.J., Huang, S.J., Lin, C.T., 2015. Dissolved organic nitrogen in wet deposition in a coastal city (Keelung) of the southern East China Sea: origin, molecular composition and flux. Atmos. Environ. 112, 20–31.

Christodoulaki, S., Petihakis, G., Kanakidou, M., Mihalopoulos, N., Tsiaras, K., Triantafyllou, G., 2013. Atmospheric deposition in the Eastern Mediterranean. A driving force for ecosystem dynamics. J. Mar. Syst. 109, 78–93.

Cornell, S.E., 2011a. Atmospheric nitrogen deposition: revisiting the question of the importance of the organic component. Environ. Pollut. 159, 2214–2222.

Cornell, S.E., 2011b. Atmospheric nitrogen deposition: revisiting the question of the invisible organic fraction. Proc. Environ. Sci. 6, 96–103.

Cornell, S.E., Mace, K., Coeppicus, S., Duce, R., Huebert, B., Jickells, T., Zhuang, L.Z., 2001. Organic nitrogen in Hawaiian rain and aerosol. J. Geophys. Res.: Atmos. 106, 7973–7983.

Dahl, E.E., Yvon-Lewis, S.A., Saltzman, E.S., 2007. Alkyl nitrate (C_1-C_3) depth profiles in the tropical Pacific Ocean. J. Geophys. Res.: Oceans 112, 1–11.

Dentener, F., Drevet, J., Lamarque, J.F., Bey, I., Eickhout, B., Fiore, A.M., Hauglustaine, D., Horowitz, L.W., Krol, M., Kulshrestha, U.C., Lawrence, M., 2006. Nitrogen and sulfur deposition on regional and global scales: a multimodel evaluation. Global Biogeochem. Cycles 20 (4).

Duce, R.A., LaRoche, J., Altieri, K., Arrigo, K.R., Baker, A.R., Capone, D.G., Cornell, S., Dentener, F., Galloway, J., Ganeshram, R.S., Geider, R.J., Jickells, T., Kuypers, M.M., Langlois, R., Liss, P.S., Liu, S.M., Middelburg, J.J., Moore, C.M., Nickovic, S., Oschlies, A., Pedersen, T., Prospero, J., Schlitzer, R., Seitzinger, S., Sorensen, L.L., Uematsu, M., Ulloa, O., Voss, M., Ward, B., Zamora, L., 2008. Impacts of atmospheric anthropogenic nitrogen on the open ocean. Science 320, 893–897.

Duce, R.A., Liss, P.S., Merrill, J.T., Atlas, E.L., Buat-Menard, P., Hicks, B.B., Miller, J.M., Prospero, J.M., Arimoto, R.C.T.M., Church, T.M., Ellis, W., 1991. The atmospheric input of trace species to the world ocean. Global Biogeochem. Cycles 5 (3), 193–259.

Facchini, M.C., Decesari, S., Rinaldi, M., Carbone, C., Finessi, E., Mircea, M., Fuzzi, S., Moretti, F., Tagliavini, E., Ceburnis, D., O'Dowd, C.D., 2008. Important source of marine secondary organic aerosol from biogenic amines. Environ. Sci. Technol. 42, 9116–9121.

Farmer, D., Cohen, R., 2008. Observations of HNO_3, ΣAN, ΣPN and NO_2 fluxes: evidence for rapid HOx chemistry within a pine forest canopy. Atmos. Chem. Phys. 8, 3899–3917.

Finlayson-Pitts, B., Pitts-Jr, J., 2000. Chemistry of the Upper and Lower Atmosphere. Academic Press, San Diego.

Fischer, E., Pszenny, A., Keene, W., Maben, J., Smith, A., Stohl, A., Talbot, R., 2006. Nitric acid phase partitioning and cycling in the New England coastal atmosphere. J. Geophys. Res.: Atmos. 111 (D23).

Galloway, J.N., Dentener, F.J., Capone, D.G., Boyer, E.W., Howarth, R.W., Seitzinger, S.P., Asner, G.P., Cleveland, C.C., Green, P.A., Holland, E.A., Karl, D.M., 2004. Nitrogen cycles: past, present, and future. Biogeochemistry 70 (2), 153–226.

Galloway, J.N., Townsend, A.R., Erisman, J.W., Bekunda, M., Cai, Z., Freney, J.R., Martinelli, L.A., Seitzinger, S.P., Sutton, M.A., 2008. Transformation of the nitrogen cycle: recent trends, questions, and potential solutions. Science 320 (5878), 889–892.

Goñi, M.A., Aceves, H.L., Thunell, R.C., Tappa, E., Black, D., Astor, Y., Varela, R., Muller-Karger, F., 2003. Biogenic fluxes in the Cariaco Basin: a combined study of sinking particulates and underlying sediments. Deep Sea Res. Oceanogr. Res. Pap. 50 (6), 781–807.

Heintzenberg, J., Covert, D.C., Van Dingenen, R., 2000. Size distribution and chemical composition of marine aerosols: a compilation and review. Tellus Ser. B Chem. Phys. Meteorol. 52, 1104–1122.

Hendry, C.D., Berish, C.W., Edgerton, E.S., 1984. Precipitation chemistry at turrialba, Costa Rica. Water Resour. Res. 20 (11), 1677–1684.

Huang, S., Arimoto, R., Rahn, K.A., 2001. Sources and source variations for aerosol at Mace Head, Ireland. Atmos. Environ. 35, 1421–1437.

Ito, A., Lin, G., Penner, J.E., 2014. Reconciling modeled and observed atmospheric deposition of soluble organic nitrogen at coastal locations. Global Biogeochem. Cycles 28 (6), 617–630.

Ito, A., Lin, G., Penner, J.E., 2015. Global modeling study of soluble organic nitrogen from open biomass burning. Atmos. Environ. 121, 103–112.

Jia, Y., Yu, G., Gao, Y., He, N., Wang, Q., Jiao, C., Zuo, Y., 2016. Global inorganic nitrogen dry deposition inferred from ground-and space-based measurements. Sci. Rep. 6.

Jickells, T., Baker, A.R., Cape, J.N., Cornell, S.E., Nemitz, E., 2013. The cycling of organic nitrogen through the atmosphere. Philos. Trans. R. Soc. Lond. B Biol. Sci. 368 (1621), 20130115.

Jickells, T.D., Buitenhuis, E., Altieri, K., Baker, A.R., Capone, D., Duce, R.A., Dentener, F., Fennel, K., Kanakidou, M., LaRoche, J., Lee, K., 2017. A reevaluation of the magnitude and impacts of anthropogenic atmospheric nitrogen inputs on the ocean. Global Biogeochem. Cycles 31 (2), 289–305.

Jickells, T.D., Kelly, S.D., Baker, A.R., Biswas, K., Dennis, P.F., Spokes, L.J., Witt, M., Yeatman, S.G., 2003. Isotopic evidence for a marine ammonia source. Geophys. Res. Lett. 30 (7).

Kanakidou, M., Duce, R.A., Prospero, J.M., Baker, A.R., Benitez-Nelson, C., Dentener, F.J., Hunter, K.A., Liss, P.S., Mahowald, N., Okin, G.S., Sarin, M., Tsigaridis, K., Uematsu, M., Zamora, L.M., Zhu, T., 2012. Atmospheric fluxes of organic N and P to the global ocean. Global Biogeochem. Cycles 26.

Kim, T.-W., Lee, K., Duce, R., Liss, P., 2014. Impact of atmospheric nitrogen deposition on phytoplankton productivity in the South China Sea. Geophys. Res. Lett. 41, 3156–3162.
Kim, T.-W., Lee, K., Najjar, R.G., Jeong, H.-D., Jeong, H.J., 2011. Increasing N abundance in the northwestern Pacific Ocean due to atmospheric nitrogen deposition. Science 334, 505–509.
Kumar, A., Sarin, M.M., 2010. Atmospheric water-soluble constituents in fine and coarse mode aerosols from high-altitude site in western India: long-range transport and seasonal variability. Atmos. Environ. 44, 1245–1254.
Lesworth, T., Baker, A.R., Jickells, T., 2010. Aerosol organic nitrogen over the remote Atlantic Ocean. Atmos. Environ. 44, 1887–1893.
Lindberg, S.E., 1982. Factors influencing trace metal, sulfate and hydrogen ion concentrations in rain. Atmos. Environ. 16 (7), 1701–1709 (1967).
Luo, L., Yao, X., Gao, H., Hsu, S., Li, J., Kao, S., 2016. Nitrogen speciation in various types of aerosols in spring over the northwestern Pacific Ocean. Atmos. Chem. Phys. 16, 325–341.
Mace, K.A., Duce, R.A., Tindale, N.W., 2003a. Organic nitrogen in rain and aerosol at Cape grim, tasmania, Australia. J. Geophys. Res.: Atmos. 108.
Mace, K.A., Kubilay, N., Duce, R.A., 2003b. Organic nitrogen in rain and aerosol in the eastern Mediterranean atmosphere: an association with atmospheric dust. J. Geophys. Res.: Atmos. 108.
Matsumoto, K., Yamato, K., 2017. Water-soluble organic nitrogen in the gas phase measured by the denuder–filter pack method. Tellus B 69 (1), 1306916.
Miyazaki, Y., Kawamura, K., Jung, J., Furutani, H., Uematsu, M., 2011. Latitudinal distributions of organic nitrogen and organic carbon in marine aerosols over the western North Pacific. Atmos. Chem. Phys. 11, 3037–3049.
Montes, E., Altabet, M., Muller-Karger, F., Scranton, M., Thunell, R., Benitez-Nelson, C., Lorenzoni, L., Astor, Y., 2013. Biogenic nitrogen gas production at the oxic–anoxic interface in the Cariaco Basin, Venezuela. Biogeosciences 10, 267–279.
Morales, J.A., Albornoz, A., Socorro, E., Morillo, A., 2001. An estimation of the nitrogen and phosphorus loading by wet deposition over Lake Maracaibo, Venezuela. Water Air Soil Pollut. 128, 207–221.
Muller-Karger, F.E., Castro, R.A., 1994. Mesoscale processes affecting phytoplankton abundance in the southern Caribbean Sea. Continent. Shelf Res. 14 (2–3), 199–221.
Muller-Karger, F., Varela, R., Thunell, R., Astor, Y., Zhang, H., Luerssen, R., Hu, C., 2004. Processes of coastal upwelling and carbon flux in the Cariaco Basin. Deep Sea Res. Part II Top. Stud. Oceanogr. 51 (10), 927–943.
Muller-Karger, F.E., Varela, R., Thunell, R.C., Scranton, M.I., Taylor, G.T., Astor, Y., Benitez-Nelson, C., Lorenzoni, L., Tappa, E., Goni, M.A., 2010. The CARIACO oceanographic time series. In: Liu, K.-K., Atkinson, L., Quinones, R., Talaue-McManus, L. (Eds.), Carbon and Nutrient Fluxes in Continental Margins: a Global Synthesis, JGOFS Continental Margins Task Team (CMTT). Springer-Verlag, Berlin Heidelberg, pp. 454.
Muller-Karger, F., Varela, R., Thunell, R., Scranton, M., Bohrer, R., Taylor, G., Capelo, J., Astor, Y., Tappa, E., Ho, T.Y., Walsh, J.J., 2001. Annual cycle of primary production in the Cariaco Basin: response to upwelling and implications for vertical export. J. Geophys. Res.: Oceans 106 (C3), 4527–4542.
Nakamura, T., Ogawa, H., Maripi, D.K., Uematsu, M., 2006. Contribution of water soluble organic nitrogen to total nitrogen in marine aerosols over the East China Sea and western North Pacific. Atmos. Environ. 40, 7259–7264.
Neff, J.C., Holland, E.A., Dentener, F.J., McDowell, W.H., Russell, K.M., 2002. The origin, composition and rates of organic nitrogen deposition: a missing piece of the nitrogen cycle? Biogeochemistry 57, 99–136.
Pacheco, M., Donoso, L., Sanhueza, E., 2004. Soluble organic nitrogen in Venezuelan rains. Tellus 56B, 393–395.
Pavuluri, C.M., Kawamura, K., Fu, P.Q., 2015. Atmospheric chemistry of nitrogenous aerosols in northeastern Asia: biological sources and secondary formation. Atmos. Chem. Phys. 15 (17), 9883–9896.
Peierls, B.L., Paerl, H.W., 1997. Bioavailability of atmospheric organic nitrogen deposition to coastal phytoplankton. Limnol. Oceanogr. 42, 1819–1823.
Prospero, J.M., Barrett, K., Church, T., Dentener, F., Duce, R.A., Galloway, J.N., Levy, H., Moody, J., Quinn, P., 1996. Atmospheric deposition of nutrients to the north Atlantic basin. Biogeochemistry 35 (1), 27–73.
Qi, J.H., Shi, J.H., Gao, H.W., Sun, Z., 2013. Atmospheric dry and wet deposition of nitrogen species and its implication for primary productivity in coastal region of the Yellow Sea, China. Atmos. Environ. 81, 600–608.
Savoie, D.L., Arimoto, R., Keene, W.C., Prospero, J.M., Duce, R.A., Galloway, J.N., 2002. Marine biogenic and anthropogenic contributions to non-sea-salt sulfate in the marine boundary layer over the North Atlantic Ocean. J. Geophys. Res. Atmos. 107 (D18), 4356.
Savoie, D.L., Prospero, J.M., 1980. Water-soluble potassium, calcium, and magnesium in the aerosols over the tropical North Atlantic. J. Geophys. Res.: Oceans 85 (C1), 385–392.
Seitzinger, S.P., Sanders, R.W., Styles, R., 2002. Bioavailability of DON from natural and anthropogenic sources to estuarine plankton. Limnol. Oceanogr. 47, 353–366.
Seinfeld, J.H., Pandis, S.N., 1998. From Air Pollution to Climate Change. Atmospheric Chemistry and Physics. John Wiley and Sons, New York.
Singh, A., Gandhi, N., Ramesh, R., 2012. Contribution of atmospheric nitrogen deposition to new production in the nitrogen limited photic zone of the northern Indian Ocean. J. Geophys. Res.: Oceans 117 (C6).
Spokes, L.J., Yeatman, S.G., Cornell, S.E., Jickells, T.D., 2000. Nitrogen deposition to the eastern Atlantic Ocean. The importance of south-easterly flow. Tellus Ser. B Chem. Phys. Meteorol. 52, 37–49.
Stark, H., Brown, S.S., Goldan, P.D., Aldener, M., Kuster, W.C., Jakoubek, R., Fehsenfeld, F.C., Meagher, J., Bates, T.S., Ravishankara, A.R., 2007. Influence of nitrate radical on the oxidation of dimethyl sulfide in a polluted marine environment. J. Geophys. Res.: Atmos. 112.
Teodoru, C.R., Friedl, G., Friedrich, J., Roehl, U., Sturm, M., Wehrli, B., 2007. Spatial distribution and recent changes in carbon, nitrogen and phosphorus accumulation in sediments of the Black Sea. Mar. Chem. 105 (1), 52–69.
Thunell, R., Benitez-Nelson, C., Varela, R., Astor, Y., Muller-Karger, F., 2007. Particulate organic carbon fluxes along upwelling-dominated continental margins: rates and mechanisms. Global Biogeochem. Cycles 21 (1), GB1022.
Trebs, I., Lara, L.L., Zeri, L.M.M., Gatti, L.V., Artaxo, P., Dlugi, R., Slanina, J., Andreae, M.O., Meixner, F.X., 2006. Dry and wet deposition of inorganic nitrogen compounds to a tropical pasture site (Rondonia, Brazil). Atmos. Chem. Phys. 6, 447–469.
Updyke, K.M., Nguyen, T.B., Nizkorodov, S.A., 2012. Formation of brown carbon via reactions of ammonia with secondary organic aerosols from biogenic and anthropogenic precursors. Atmos. Environ. 63, 22–31.
Violaki, K., Mihalopoulos, N., 2010. Water-soluble organic nitrogen (WSON) in size-segregated atmospheric particles over the Eastern Mediterranean. Atmos. Environ. 44 (35), 4339–4345.
Violaki, K., Sciare, J., Williams, J., Baker, A., Martino, M., Mihalopoulos, N., 2015. Atmospheric water soluble organic nitrogen (WSON) over marine environments: a global perspective. Biogeosciences 12 (10), 3131–3140.
Violaki, K., Zarbas, P., Mihalopoulos, N., 2010. Long-term measurements of dissolved organic nitrogen (DON) in atmospheric deposition in the Eastern Mediterranean: fluxes, origin and biogeochemical implications. Mar. Chem. 120, 179–186.
Wedyan, M., Fandi, K.G., Al-Rousan, S., 2007. Bioavailability of atmospheric dissolved organic nitrogen in the marine aerosol over the Gulf of Aqaba. Aust. J. Basic and Appl. Sci. 1, 208–212.
Zamora, L.M., Prospero, J.M., Hansell, D.A., 2011. Organic nitrogen in aerosols and precipitation at Barbados and Miami: implications regarding sources, transport and deposition to the western subtropical North Atlantic. J. Geophys. Res.: Atmos. 116.
Zhang, Y., Zheng, L., Liu, X., Jickells, T., Cape, J.N., Goulding, K., Fangmeier, A., Zhang, F., 2008. Evidence for organic N deposition and its anthropogenic sources in China. Atmos. Environ. 42, 1035–1041.
Zhao, Y., Zhang, L., Pan, Y., Wang, Y., Paulot, F., Henze, D.K., 2015. Atmospheric nitrogen deposition to the northwestern Pacific: seasonal variation and source attribution. Atmos. Chem. Phys. 15, 10905–10924.